

An endocytosis defect as a possible cause of proteinuria in polycystic kidney disease

NICHOLAS OBERMÜLLER,¹ BETTINA KRÄNZLIN,¹ WERNER F. BLUM,²
NORBERT GRETZ,¹ AND RALPH WITZGALL³

¹Medical Research Center, Klinikum Mannheim, University of Heidelberg, 68167 Mannheim; ²Lilly Deutschland, 61350 Bad Homburg, and University Children's Hospital, 35392 Giessen; and

³Institute for Anatomy and Cell Biology I, University of Heidelberg, 69120 Heidelberg, Germany

Received 5 April 2000; accepted in final form 10 October 2000

Obermüller, Nicholas, Bettina Kränzlin, Werner F. Blum, Norbert Gretz, and Ralph Witzgall. An endocytosis defect as a possible cause of proteinuria in polycystic kidney disease. *Am J Physiol Renal Physiol* 280: F244–F253, 2001.—Because proteinuria has been demonstrated in patients with autosomal-dominant polycystic kidney disease (ADPKD), we have investigated whether proteinuria also occurs in the (*cy/+*) rat, a widely used model for ADPKD. Increased urinary excretion of proteins, in particular of albumin, can be found in 16-wk-old (*cy/+*) rats, with a gel electrophoresis pattern compatible with a tubular origin of proteinuria. Using FITC-labeled dextran as an *in vivo* tracer for renal tubular endosomal function, we could show that portions of cyst-lining epithelia from proximal tubules have lost the ability to endocytose, which is necessary for the reabsorption of low-molecular-weight proteins. By immunohistochemistry, the expression of other proteins implicated in endocytosis, such as the chloride channel CIC-5 and the albumin receptor megalin, correlated well with the presence and absence of FITC-dextran in cysts. As an example of growth factor systems possibly being affected by this endocytosis defect, we could detect increased urinary levels of insulin-like growth factor-I protein in (*cy/+*) animals. These data indicate that proteinuria and albuminuria in the aforementioned rat model for ADPKD are due to a loss of the endocytic machinery in epithelia of proximal tubular cysts. This may also affect the concentration of different growth factors and hormones in cyst fluids and thus modulate cyst development.

CIC-5; megalin; fluorescein isothiocyanate-dextran; albuminuria; proteinuria; insulin-like growth factor-I

AUTOSOMAL-DOMINANT POLYCYSTIC kidney disease (ADPKD) can be considered as one of the most prevalent tubulointerstitial diseases; it is characterized by the formation of multiple cysts and considerable enlargement of both kidneys. Although it has now been established that mutations in the *PKD1* (13a) and *PKD2* (27) genes are responsible for most ADPKD cases, there is a high degree of variability in the clinical course of those patients.

Several factors have been considered as being of prognostic value in patients suffering from ADPKD. Importantly, the occurrence of proteinuria and albuminuria has been implicated in a more severe disease progression in ADPKD patients (6, 38). Although there is evidence that human ADPKD may affect all segments of the nephron, including the proximal tubule (4, 10, 14), it has not been addressed whether alterations of this nephron segment contribute to proteinuria and albuminuria. The (*cy/+*) rat, an animal model for ADPKD, provides a suitable tool for an investigation of the contribution of impaired tubular function to proteinuria and albuminuria, because in this strain cysts originate predominantly from the proximal tubule (8, 31, 37).

Low-molecular-weight plasma proteins such as albumin and β_2 -microglobulin are reabsorbed via a receptor-mediated endocytosis pathway by proximal tubules and are then delivered to lysosomes for degradation (25). The luminal uptake of albumin requires the presence of binding proteins such as megalin (gp330) as the first step in the endocytic cascade (9). The transport of albumin and other low-molecular-weight proteins into endocytic vesicles also depends on the appropriate endosomal acidification, which is accomplished by the transport of protons through a V-type H^+ -ATPase (25). For the supply of the required amounts of counterions, channels like the recently discovered chloride channel CIC-5 are indispensable to guarantee the appropriate chloride influx into endosomes (17, 25). Defective CIC-5 function caused by mutations in the respective gene therefore leads to impaired endosomal acidification and consequently to low-molecular-weight proteinuria, as found in Dent's disease and related syndromes (22, 23).

In this study we show that, similar to the situation in human patients (6, 38, 44), increased proteinuria and albuminuria can be observed in (*cy/+*) rats. By the administration of FITC-labeled dextran as an *in vivo* marker for endocytosis in the proximal tubule, in combination with the immunohistochemical analysis of

Address for reprint requests and other correspondence: R. Witzgall, Institute for Anatomy and Cell Biology I, Univ. of Heidelberg, Im Neuenheimer Feld 307, 69120 Heidelberg, Germany (E-mail: ralph.witzgall@urz.uni-heidelberg.de).

The costs of publication of this article were defrayed in part by the payment of page charges. The article must therefore be hereby marked "advertisement" in accordance with 18 U.S.C. Section 1734 solely to indicate this fact.

CIC-5 and the multifunctional receptor megalin, we provide evidence that the partial loss of endocytosis in cysts of (*cy/+*) rat kidneys contributes to the increased excretion of urinary proteins. We also demonstrate that the impaired tubular endocytic capacity leads to increased urinary excretion of insulin-like growth factor-I (IGF-I). Prolonged exposure of cysts to increased luminal growth factor concentrations may play a secondary role in the enlargement of renal cysts.

MATERIALS AND METHODS

Animals. Our colony of (*cy/+*) rats is derived from the Han:SPRD rat strain. It has been inbred for over 20 generations in Mannheim, Germany, and has therefore been registered as follows: polycystic kidney disease, Mannheim (PKD/Mhm; Inbred Strains of Rats, <http://www.informatics.jax.org/external/festing/rat/docs/PKD.shtml>). Animals were maintained under the control of N. Gretz at the Animal Care Facility in Mannheim. Sixteen-week-old male heterozygous and wild-type animals as well as normal Sprague-Dawley rats were chosen for the different experimental procedures. All rats were allowed free access to tap water and to rat chow containing 19% protein.

Infusion of FITC-labeled dextran and tissue preparation. FITC-labeled anionic dextran (molecular mass = 10 kDa, catalog no. D-1821) was purchased from Molecular Probes (Leiden, The Netherlands). Rats were deeply anesthetized with ketamine (100 mg/kg) and xylazine (5 mg/kg) before a midline incision was made to locate the abdominal aorta below the renal arteries. Several drops of 0.9% NaCl were administered to the peritoneal cavity to balance the fluid loss caused by evaporation. Next, the right jugular vein was carefully dissected free, and FITC-labeled dextran (1,75 mg/100 g body wt, dissolved in 0.5 ml 0.9% NaCl) was injected as a bolus into the right jugular vein over a period of 30 s. Typically, a green discoloration of the bladder could be observed after 2 min. Six minutes after the injection of the FITC-dextran bolus, the infrarenal abdominal aorta was cannulated and the rats were subjected to perfusion-fixation for subsequent visualization of FITC-labeled dextran and immunohistochemistry. Animals were perfused with 2% freshly depolymerized paraformaldehyde in PBS, pH 7.4, at a pressure level of 180 mm Hg for 3 min and subsequently with a 18% sucrose solution in PBS for another 3 min at the same pressure level. Next, kidneys were removed, cut into slices, and incubated in a 18% sucrose-PBS solution (containing 0.02% sodium azide) for another 24 h at 4°C. Tissues were then snap-frozen in liquid nitrogen-cooled isopentane and stored at -80°C until further use. Rats without administration of FITC-dextran were perfused in a similar way, and both kidneys were processed as described above.

Histomorphological analysis of FITC-dextran uptake and immunohistochemistry. Five- to seven-micrometer cryostat sections from FITC-dextran-infused rat kidneys were transferred onto silane-coated glass slides, air-dried, washed for 30 min in PBS, and mounted in bicarbonate-buffered glycerol (pH 8.6) before being analyzed under the fluorescence microscope.

For additional immunohistochemical experiments, cryostat sections from FITC-dextran-infused rat kidneys were washed in PBS and incubated for 30 min at room temperature in a blocking solution consisting of 2% BSA in PBS. The sections were then incubated with the following primary antibodies diluted in blocking solution as indicated: an affinity-purified rabbit polyclonal antibody against the COOH

terminus of rat CIC-5 (diluted 1:200; kind gift of T. Jentsch, Hamburg, Germany) (17); a mouse monoclonal anti-megalina antibody (diluted 1:300; kind gift of D. Kerjaschki, Vienna, Austria) (20); and a mouse monoclonal antibody against dipeptidyl peptidase IV (diluted 1:500; kind gift of W. Reuter, Berlin, Germany) (19).

The antibodies were applied for 2 h at room temperature and subsequently overnight at 4°C. The next day, slides were rinsed in PBS and incubated with the appropriate Cy3-coupled secondary antibodies (Dianova, Hamburg, Germany). For double-labeling experiments on noninfused rat kidneys, two primary antibodies developed in different species were applied together, followed by the simultaneous detection using FITC- and Cy3-coupled secondary antibodies.

Blood pressure measurements and assessment of blood and urine chemistry. Systolic blood pressure values were monitored by tail plethysmography in awake, trained animals. Sixteen-week-old (*cy/+*) and (*+/+*) rats ($n = 5/\text{group}$) were placed into metabolic cages to collect 24-h urine samples. Blood samples were obtained from all animals from the retroorbital plexus under short anesthesia. The (*cy/+*) or (*+/+*) carrier status was verified by the histological examination of the kidneys.

Determination of urinary protein and albumin levels. Before protein measurements were taken, all samples were centrifuged for 2 min at 14,000 *g*, and the supernatants were collected. Protein concentrations were determined according to an improved Bradford method (48) using the Bio-Rad protein assay kit (Bio-Rad, Munich, Germany) with BSA as a standard.

The concentration of albumin in rat urine was determined by using a competitive two-step ELISA, which was developed at the Medical Research Center in Mannheim. During the first step, a chicken anti-rat albumin antibody (catalog no. 55727, Cappel, Eppelheim, Germany) was incubated with the sample. After complexes between albumin and the anti-rat albumin antibody had formed, this mixture was transferred to a 96-well plate coated with rat albumin (catalog no. A-4538, Sigma, Deisenhofen, Germany). The amount of antibody bound to the albumin in the 96-well plates was determined with a peroxidase-coupled antibody directed against chicken IgG (catalog no. A-9792, Sigma) and subsequent enzymatic reaction. The concentration of the reaction product was measured photometrically at 450 nm. Each measurement included rat albumin samples with known concentrations, so that the albumin concentration in the urine could be determined from a standard curve.

Measurement of urinary IGF-I protein by radioimmunoassay. Urinary IGF-I levels were determined by radioimmunoassay as described previously (5, 43).

Nonreducing SDS-PAGE of urinary proteins. Equal urine volumes (35 μl , corresponding to 5.5–38.0 μg of protein) were combined with 17.5 μl of 3 \times SDS-sample buffer (1 \times SDS-sample buffer is 125 mM Tris·HCl, pH 6.7, 2.5% SDS, 10% glycerol, and 0.01% bromophenol blue), boiled, and loaded onto a denaturing polyacrylamide gel. A broad-range protein marker (New England Biolabs, Schwalbach, Germany) was used as a molecular weight standard. Electrophoresis was followed by staining of the gel with Coomassie brilliant blue R250 for 1 h. The gels were destained, washed in double distilled water, and dried in a cellophane membrane for storage.

Preparation of total RNA. The kidneys from 16-wk-old male (*cy/+*) and (*+/+*) rats were rapidly removed, and total RNA was extracted according to the acid guanidinium-phenol-chloroform protocol of Chomczynski and Sacchi (7). The resulting RNA pellets were dissolved in diethylpyrocarbon-

Table 1. Blood pressure levels, serum, and urine parameters of 16-wk-old male (*cy/+*) and (*+/+*) rats

	(<i>cy/+</i>) (n = 5)	(<i>+/+</i>) (n = 5)	P Value
Serum creatinine, mg/dl	0.81 ± 0.13	0.46 ± 0.18	0.008*
Serum urea, mg/dl	96.4 ± 12.6	56.0 ± 25.0	0.012*
Systolic blood pressure, mm Hg	123.4 ± 9.7	124.4 ± 5.9	0.850
Protein excretion, mg/24 h	50.2 ± 15.9	20.0 ± 5.6	0.004*
Albumin excretion, mg/24 h	13.1 ± 6.3	3.1 ± 1.3	0.022*

Values are as means ± SD. n, No. of rats. *Statistically significant at $P \leq 0.05$.

ate-treated water, and the yield was measured by spectrometry at 260 nm. Samples were stored at -80°C until further use. The integrity of the extracted RNA was checked by agarose gel electrophoresis.

Ribonuclease protection assay for renal IGF-I mRNA. RNase protection analysis was performed according to standard protocols (3). A 205-bp rat IGF-I cDNA fragment (kind gift of Derek LeRoith, National Institutes of Health, Bethesda, MD) (1) and an 80-bp 18S cDNA fragment (Ambion, Austin, TX) were used for in vitro transcription. Plasmids were digested appropriately, and radiolabeled antisense cRNA probes were synthesized in vitro with T7 RNA polymerase (Roche Molecular Biochemicals, Mannheim, Germany) in the presence of [α - ^{32}P]UTP.

Fifty micrograms of total RNA were hybridized with the radiolabeled IGF-I riboprobe, whereas 50 ng of total RNA were hybridized with the radiolabeled 18S riboprobe; tRNA served as a negative control. Hybridization was conducted overnight at 42°C . After digestion with RNase A and T1, the protected fragments were separated on a 4% polyacrylamide/6 M urea gel. Thereafter, the gel was dried for 2 h, exposed for 10 min-4 days, and analyzed in a Fujifilm BAS-2500 bioimaging phosphor analyzer. Imaging plates were analyzed by using the BASReader software program and the AIDA software Image analyzing system (version 2.0, Raytest Isotopenmessgeräte, Straubenhardt, Germany).

Processing of images and gels. Black and white photographs from interference-phase contrast pictures and immunofluorescence-labeled kidney sections were scanned with a Nikon Coolscan LS-2000 by using Silverfast 4.1 software (LaserSoft, Kiel, Germany). Gels were scanned with a Linotype Saphir ultras Scanner using Linocolor 5.1 software. All files were then processed with Photoshop 5.0 (Adobe Systems, San Jose, CA).

Statistics. Statistical evaluation was performed by using the statistical analysis system (SAS Institute, Cary, NC). The procedure PROC TTEST was applied to calculate mean, SD, and *t*-test statistics.

RESULTS

In the present study, 16-wk-old male (*cy/+*) and (*+/+*) rats were analyzed with respect to urinary protein and albumin excretion. Table 1 demonstrates that there is a statistically significant increase in the mean 24-h urinary protein excretion in the (*cy/+*) group compared with that of the (*+/+*) group. Similarly, (*cy/+*) rats excreted higher levels of albumin than (*+/+*) rats (Table 1). Serum creatinine and urea values were already significantly higher in (*cy/+*) animals than in their (*+/+*) littermates, whereas no differences be-

tween the two groups could be seen with respect to the systolic blood pressure levels (Table 1).

Coomassie blue-stained protein gels of the individual urine samples run under nonreducing conditions are shown in Fig. 1. All samples obtained from (*cy/+*) animals showed stronger bands for albumin than the corresponding urine from the (*+/+*) rats, confirming the results obtained with the ELISA. The urine from (*cy/+*) rats provided no evidence for a pronounced increase in the excretion of large proteins such as immunoglobulins, which should have been present in the 150-kDa range, thus pointing against a glomerular lesion as the cause of proteinuria. Because these data suggested a tubular defect, the role of impaired endocytosis in this nephron segment was addressed more closely in subsequent experiments.

In Fig. 2a the uptake of filtered FITC-labeled dextran, which is used as a marker for endosomes (21), can be seen in normal proximal tubular cells, where it is

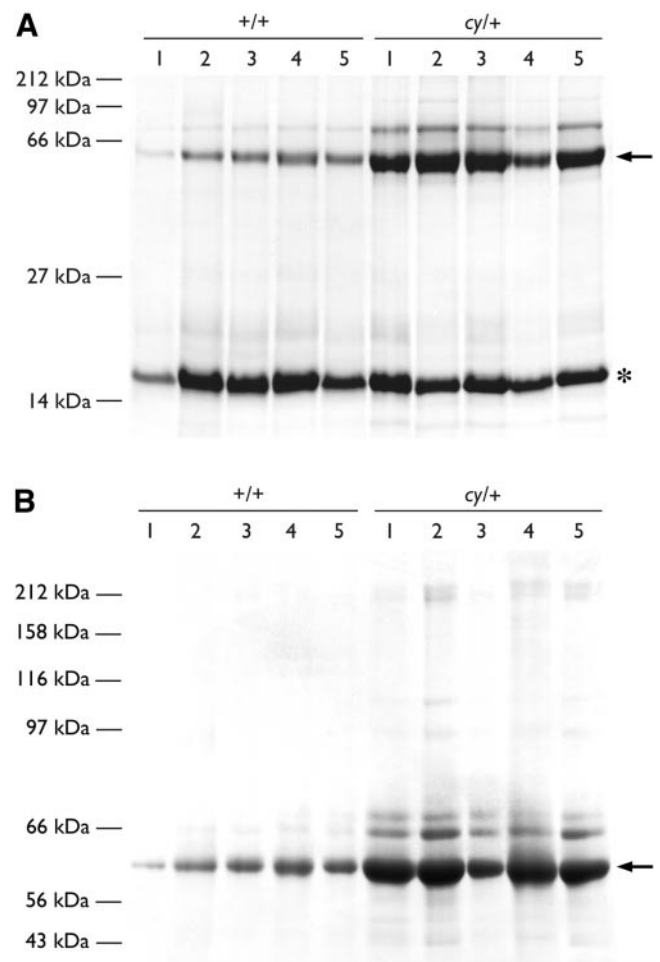


Fig. 1. Size distribution of urinary proteins from (*cy/+*) and (*+/+*) rats. Urinary proteins from 5 (*+/+*) rats and 5 (*cy/+*) rats were separated on denaturing, nonreducing gels and visualized with Coomassie blue [14% gel (A), 7% gel (B)]. The urine was obtained from the same animals, values of which are shown in Table 1 and Fig. 7. All 10 lanes were loaded with equal volumes of urine. Arrows, albumin; *, male-specific proteins (2). Please note that in B, lanes 3 and 4 have been loaded in reverse order of those in A.

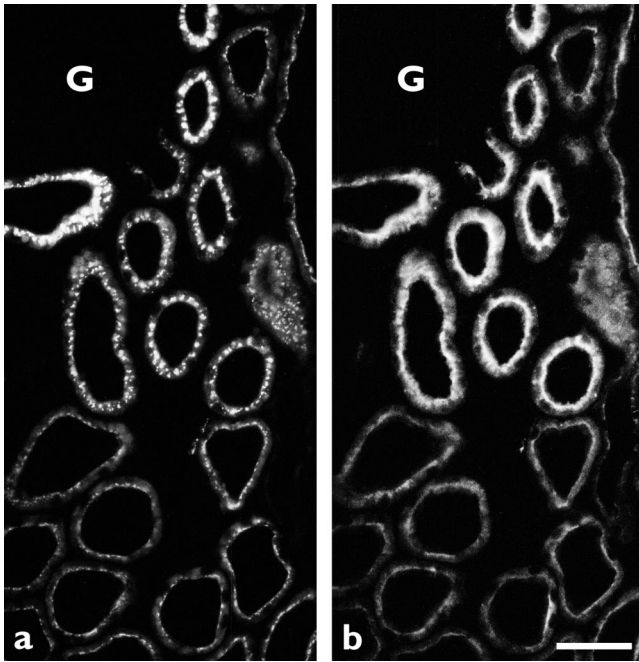


Fig. 2. Distribution of endocytosed FITC-labeled dextran and the chloride channel ClC-5 in a normal adult rat kidney. An overview of the corticomedullary border shows the strong apical labeling with FITC-dextran in the convoluted portion (*top*) and the more moderate staining in the S3 segment (*bottom*) of proximal tubular profiles (*a*). Subsequent labeling of the same section with an antibody against the chloride channel ClC-5 (*b*) demonstrates colocalization of both signals in the proximal tubules. G, glomerulus. Bar, 40 μ m.

located in a punctate fashion in the apical cytoplasm. The resulting fluorescence appears stronger in the epithelial cells of the proximal convoluted tubules than in cells of the pars recta (S3 segment), indicating a higher rate of endocytosis in the S1 and S2 segments. Immunohistochemical analysis of the same sections with an antibody against the chloride channel ClC-5, which recently has been localized to endosomes, yielded a strikingly similar distribution pattern regarding the staining intensity within different segments of the proximal tubule (Fig. 2*b*). Somewhat surprisingly, however, the distribution of ClC-5 appeared more homogeneous, whereas that of FITC-dextran was clearly punctate. This finding may be due to the fact that ClC-5 is present in many endosomal vesicles, which the light microscope will not be able to resolve into distinct entities. FITC-dextran, however, has to be reabsorbed from the tubular fluid and is therefore present in only that subset of endosomes, which has just been formed, thus resulting in a punctate appearance.

For a comprehensive analysis, double-labeling immunohistochemical experiments in normal adult rat kidneys were carried out with the anti-ClC-5 antibody and an antibody against the enzyme dipeptidyl peptidase IV, which serves as a marker for the brush border of the proximal tubule (19). Figure 3 shows that the ClC-5 protein is expressed in the apical cytoplasm just below the brush border without any overlap with dipeptidyl peptidase IV (Fig. 3, *a-d*). The intracellular distribution of internalized FITC-dextran and of the

ClC-5 chloride channel was investigated at a higher magnification and revealed a colocalization of the two signals in proximal convoluted tubules (Fig. 3, *e-h*). Only rarely, some FITC-dextran-containing vesicles did not colocalize with ClC-5. Thus there is an apparent overlap of both endosomal markers in the proximal tubule.

In (*cy/+*) rat kidneys, infusion of FITC-labeled dextran resulted in an uptake into the apical cell compartment of noncystic proximal tubules, comparable to the situation in control kidneys. However, in cystically modified proximal tubules, many cyst-lining cells did not show an uptake of FITC-labeled dextran, whereas in other epithelial cells of the same cyst, endocytosed FITC-labeled dextran was readily detectable (Figs. 4*a* and 5*a*). There was a clear variability between cysts, with some showing endocytosed FITC-labeled dextran in only a few or no epithelial cells, whereas other cysts demonstrated FITC-dextran in almost every epithelial cell. Subsequent immunohistochemical staining of the sections with the anti-ClC-5 antibody showed complete overlap with the FITC-dextran-containing cells, whereas the cyst-lining epithelia, which did not internalize FITC-labeled dextran, also did not express ClC-5 (Fig. 4*b*). Next, the presence of gp330/megalín, which has been proposed as a multiligand receptor for a variety of proteins including albumin (9, 46), was analyzed by immunohistochemistry on FITC-dextran-infused (*cy/+*) rat kidneys. In cysts, the megalín-expressing tubular cells largely colocalized with those cells that had endocytosed FITC-labeled dextran. Cells that did not express megalín were also devoid of FITC-labeled dextran (Fig. 5). At a higher magnification it could be clearly seen that it was the more flattened epithelium of the cyst walls that did not express ClC-5 and megalín any longer (Fig. 6).

The impaired endocytosis in cysts of the proximal tubule might be of functional relevance because a variety of proteins are quantitatively reabsorbed along this nephron segment. For instance, several circulating hormones and growth factors are filtered and delivered to the proximal tubule, where binding and uptake play a critical role in their metabolism (15). By the use of a specific radioimmunoassay for rat IGF-I (5, 43), we have found increased urinary excretion of IGF-I in (*cy/+*) rats compared with the respective controls (Fig. 7). To assess whether the increased amounts of urinary IGF-I protein were derived from circulating IGF-I or of renal origin, 16-wk-old (*cy/+*) as well as (*+/+*) rats were analyzed by using a RNase protection assay. In three (*+/+*) kidneys, abundant IGF-I mRNA could be detected, whereas in five kidney samples prepared from (*cy/+*) rats the corresponding protected bands were weaker (2 animals) or virtually absent (3 animals) even after a prolonged exposure (Fig. 8). These results indicate that in (*cy/+*) rat kidneys IGF-I mRNA is expressed at clearly lower levels than in unaffected (*+/+*) kidneys, therefore making it unlikely that cystic kidneys are the origin of increased urinary IGF-I protein levels.

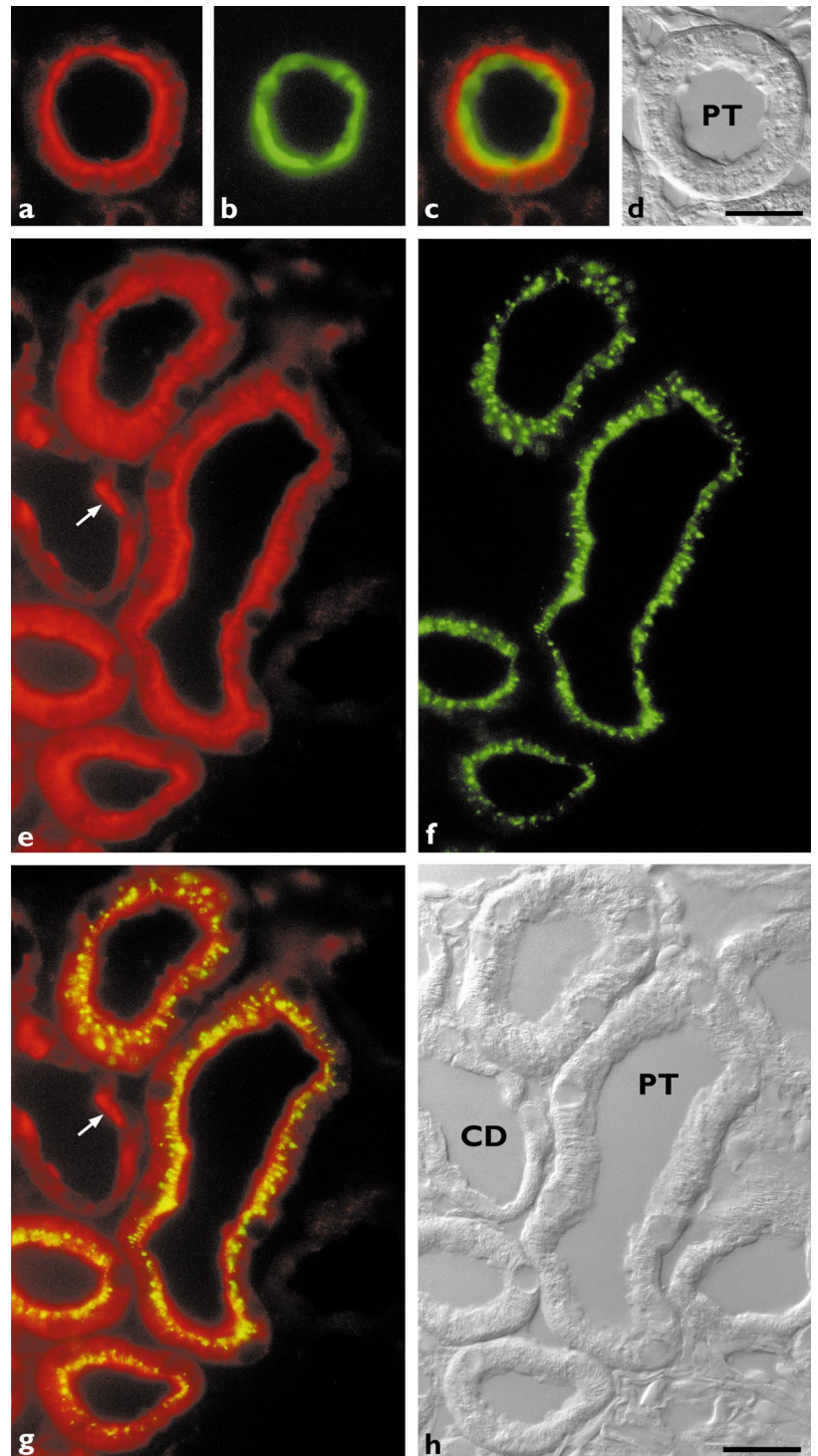


Fig. 3. Subcellular localization of the chloride channel ClC-5 in the proximal tubule. (PT; *a-d*) Double-immunofluorescence staining with antibodies against ClC-5 (*a*) and against the brush-border enzyme dipeptidyl peptidase IV (*b*) in a proximal convoluted tubule of an adult rat kidney demonstrates that the ClC-5 protein is exclusively located below the brush border (*c*; also compare the corresponding interference phase-contrast view in *d*). *e-h*: Staining of a FITC-dextran-labeled PT (*f*) with the anti-ClC-5 antibody (*e*) demonstrates a large overlap of both fluorescent signals (*g*; also compare the corresponding interference phase-contrast view in *h*). Collecting ducts (CD) also show expression of ClC-5 in intercalated cells (arrows in *e* and *g*). Bars, 20 μm .

DISCUSSION

Proteinuria has been identified as a key factor for the prognosis of renal disorders (45), and the occurrence of proteinuria has also been evaluated in ADPKD patients, where it seems to be associated with a more aggressive course of the disease (6, 38). Massive alterations of the tubulointerstitium occur during cyst development, and it is therefore important to address the role of impaired tubular function in the development of

proteinuria and albuminuria. Net urinary excretion of filtered proteins critically depends on the structural integrity of the proximal tubule, where most of the proteins are reabsorbed by endocytosis (25). Because in the (*cy/+*) rat cysts originate predominantly from the proximal tubule (8, 31, 37) and because cyst-lining epithelial cells show distinct changes such as the loss of transporters and channels (31), we focused our attention on this particular animal model of ADPKD. In-

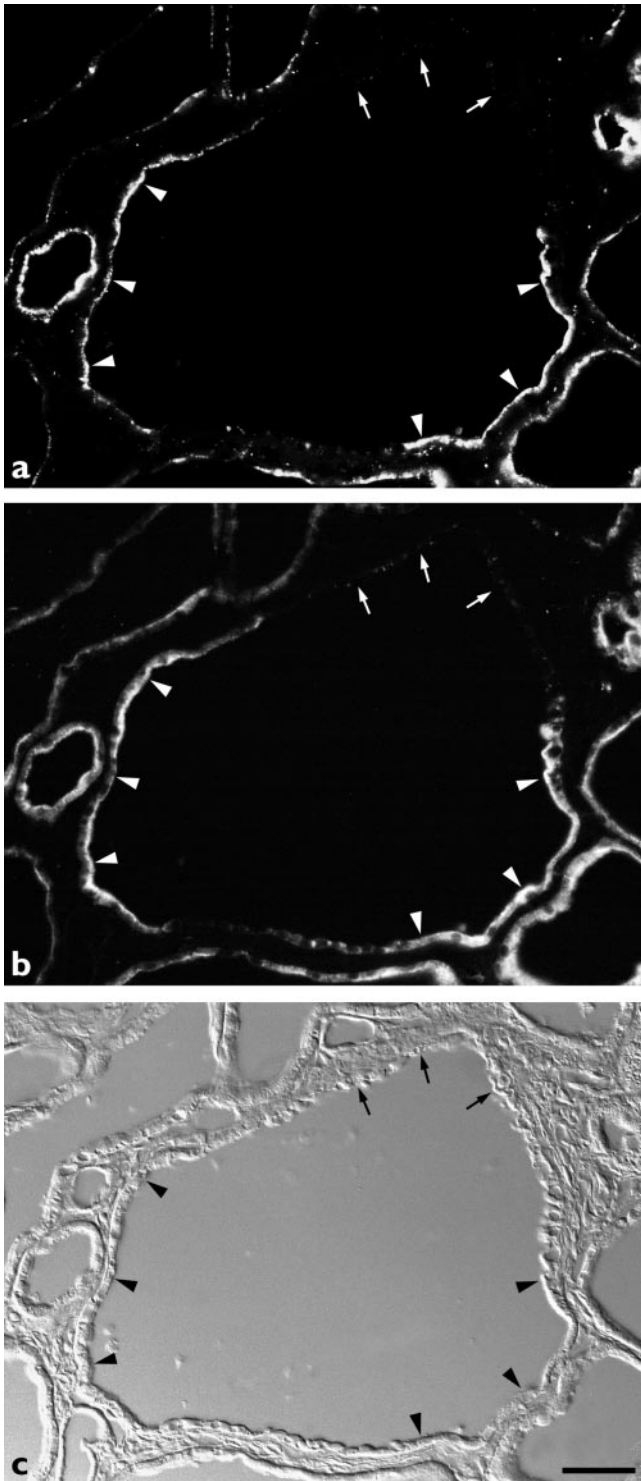


Fig. 4. FITC-dextran uptake and CIC-5 expression in cyst wall epithelia. *a*: Kidney section of a 16-wk-old (*cy/+*) rat injected with FITC-labeled dextran shows cysts with a mosaic uptake of this endocytosis marker. Arrowheads, positive areas; arrows, endocytosis-deficient areas. *b*: Immunofluorescence staining with an antibody against CIC-5 demonstrating the lack of CIC-5 expression in endocytosis-deficient cyst-lining cells, whereas FITC-dextran-positive cells still express CIC-5. *c*: Corresponding interference phase-contrast view. Bar, 50 μ m.

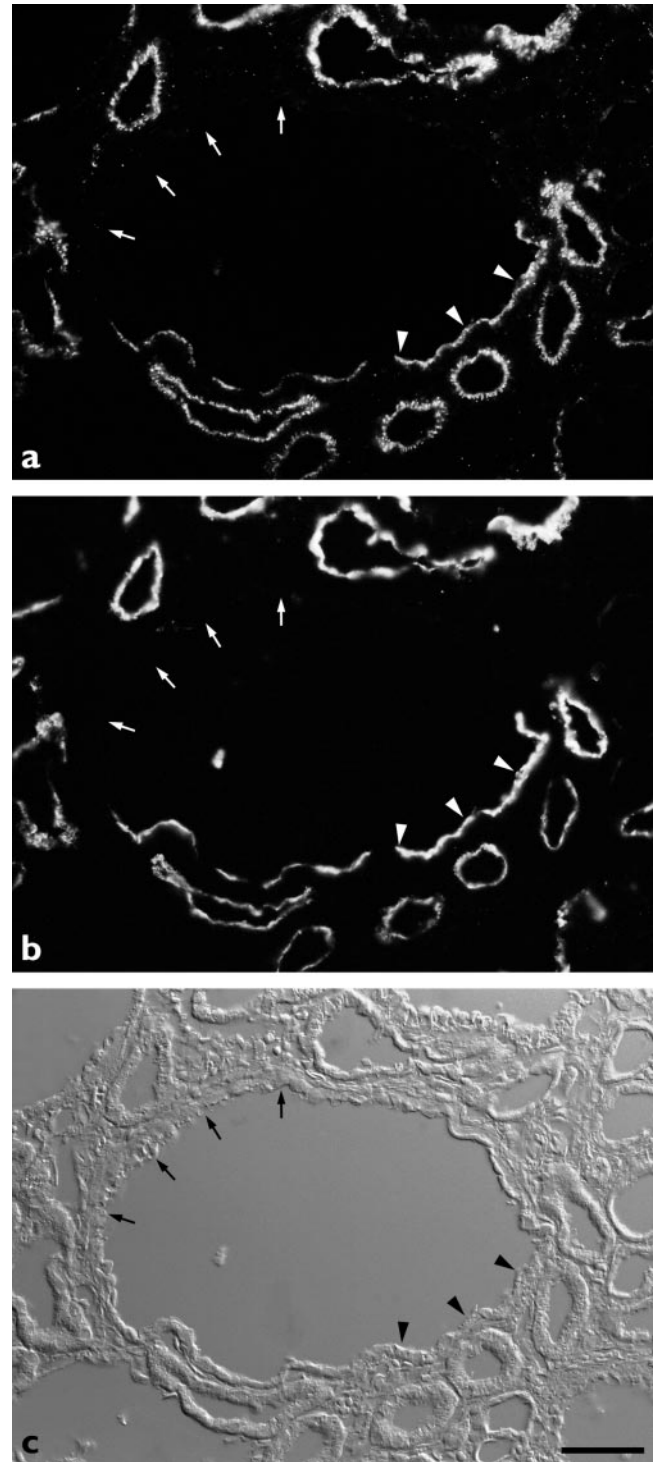


Fig. 5. FITC-dextran uptake and megalin expression in cyst wall epithelia. *a*: Kidney section of a 16-wk-old (*cy/+*) rat injected with FITC-labeled dextran shows cysts with a mosaic uptake of this endocytosis marker. Arrowheads, positive areas; arrows, endocytosis-deficient areas. *b*: Immunofluorescence staining with an antibody against megalin demonstrating the lack of megalin expression in endocytosis-deficient cyst-lining cells, whereas FITC-dextran-positive cells still express megalin. *c*: Corresponding interference phase-contrast view. Bar, 50 μ m.

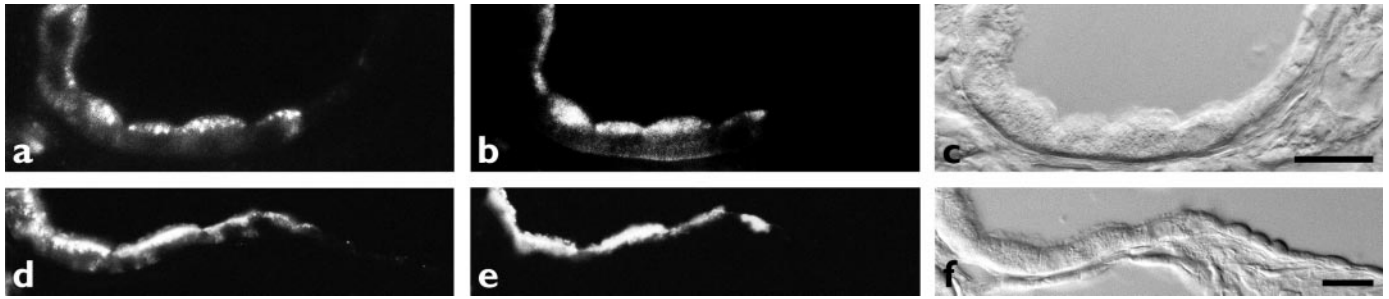


Fig. 6. FITC-dextran uptake and expression of ClC-5 and megalin in cyst wall epithelia. Higher magnification demonstrates that those areas of cyst walls, which do not endocytose FITC-dextran (*a, d*) and are not stained with the anti-ClC-5 (*b*) and anti-megalin (*e*) antibodies, are lined by a flattened epithelium. *c* and *f*: Corresponding interference phase-contrast views. Bars, 20 μ m.

deed, we were able to show an increased proteinuria, which was accompanied by albuminuria but not by a pronounced excretion of higher molecular weight proteins such as immunoglobulins. In addition to increased levels of albumin, we also found proteins of ~70 kDa in the urine of the (*cy/+*) rat, which may not be too surprising considering the fact that normal rats also excrete proteins in that size range (2).

Because those initial observations pointed to a tubular defect, they were followed up by an *in vivo* approach using FITC-labeled dextran as a fluorescent tracer for endocytosis in proximal tubules (21). Our results clearly show that portions of cyst-lining epithelia of (*cy/+*) rat kidneys have lost the ability for endocytosis. These findings were extended by demonstrating that the absence of endocytic function is paralleled by the

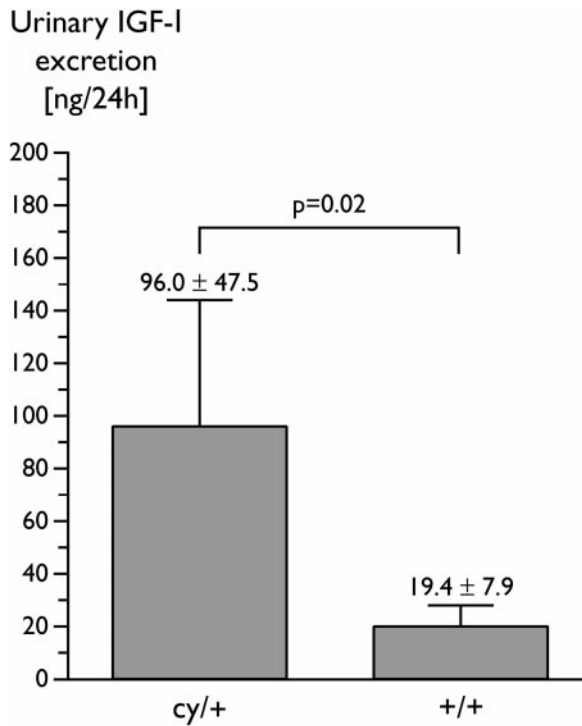


Fig. 7. Urinary excretion of insulin-like growth factor-I (IGF-I) protein. When the daily excretion of IGF-I protein in the urine was determined by radioimmunoassay, a significant difference was found between (*cy/+*) and (*+/+*) rats. Values are means \pm SD.

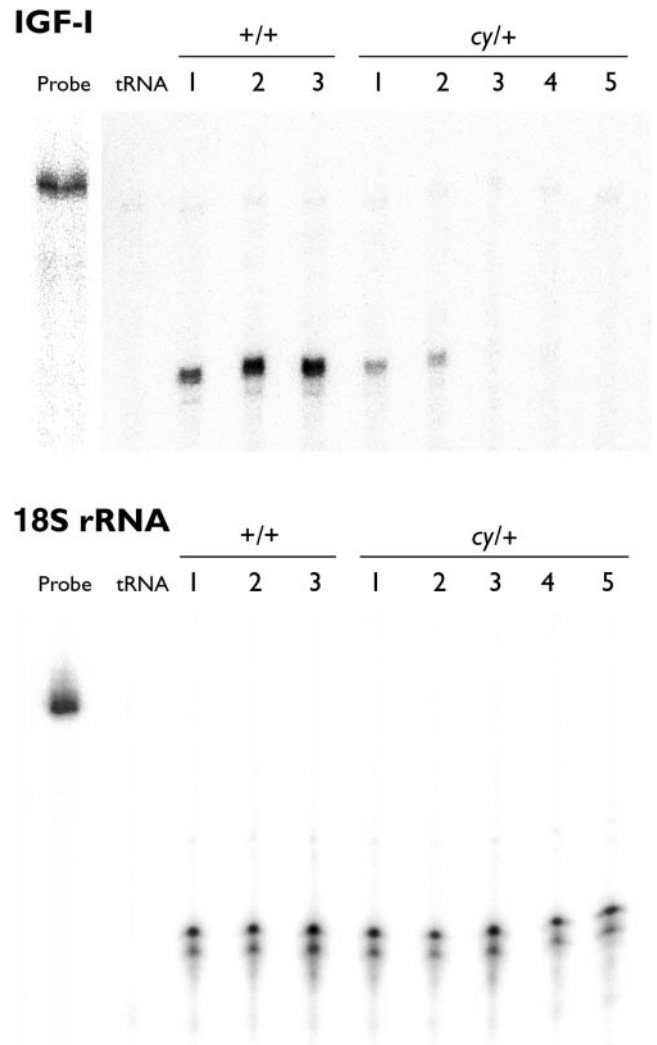


Fig. 8. The expression of IGF-I mRNA (*top*) is decreased in (*cy/+*) rat kidneys. RNase protection analysis of IGF-I mRNA in 16-wk-old (*cy/+*) and (*+/+*) rat kidneys demonstrates the strong expression of IGF-I mRNA in kidneys of 3 (*+/+*) animals (*top left*), whereas in 5 (*cy/+*) kidneys the expression is considerably weaker (*top right*). To demonstrate that the RNA concentration was determined correctly, a RNase protection assay was also performed with a radiolabeled anti-sense fragment directed against the 18S rRNA (*bottom*). Hybridization with tRNA served as a negative control. Probe, undigested anti-sense fragments.

lack of components crucially involved in the endocytic pathway, such as the putative albumin receptor megalin and the endosomal chloride channel CIC-5, in cyst-lining epithelia. A glomerular lesion as the cause of proteinuria is unlikely because of the absence of high-molecular-weight proteins in the urine; furthermore, we could not detect an increase in the systolic blood pressure levels of (*cy/+*) rats, which may result in hypertensive damage of the glomerular filtration barrier [(37) and this study]. Therefore, the urinary loss of proteins, and especially that of albumin, from cystic kidneys can best be explained as a consequence of disturbed proximal tubular function, i.e., the loss of components of the endocytic machinery, in cyst wall epithelia. In this context it should also be pointed out that in the (*cy/+*) model the cysts develop predominantly in the cortical portion of the proximal tubule (8, 31, 37), which is also the site with the highest abundance of endocytosed FITC-labeled dextran and the strongest expression of CIC-5 protein. It is conceivable that the loss of at least some proteins could be balanced by the upregulation of endocytosis in the S3 segment, limiting tubular proteinuria to a certain degree. For albumin, however, it has been suggested that an increased load cannot be handled adequately by the proximal tubule, so that a reduced reabsorption capacity may inevitably lead to albuminuria (24).

The importance of the chloride channel CIC-5 and the multifunctional clearance receptor megalin for protein reabsorption in the proximal tubule can also be appreciated by the phenotypes resulting from the inactivation of their respective genes. In Dent's disease and related syndromes, in which the function of the whole proximal tubule is compromised by a germline mutation in the gene encoding CIC-5 (22, 23), excessive low-molecular-weight proteinuria is a prominent feature of the disease. Similarly, proximal tubules from megalin-knockout mice show a reduction of endosomes and lysosomes, which is also accompanied by low-molecular-weight proteinuria (29).

The present results regarding the cellular localization of the CIC-5 protein in (*cy/+*) and (*+/+*) rat kidneys are in general agreement with previous investigations in normal human, mouse, and rat kidneys. Our own *in situ* hybridization study has shown the expression of CIC-5 mRNA in intercalated cells of connecting tubules and collecting ducts (30), which was confirmed subsequently both by others (11, 17, 36) and by this study using anti-CIC-5 antibodies. Using nonradioactive *in situ* hybridization, we could not, however, unambiguously detect CIC-5 mRNA in the proximal tubule (30), which is in contrast to our present study and previous results obtained with anti-CIC-5 antibodies (11, 17, 36). This discrepancy can probably be explained by the lower sensitivity achieved with the nonradioactive *in situ* hybridization technique. On a subcellular level, the localization of the CIC-5 protein in endosomes has been demonstrated biochemically (11, 36), ultrastructurally (17, 36), and by double staining with endosomal markers (17) and endocytosed β_2 -microglobulin, α_2 -macroglobulin, and albumin (11, 17).

We are able to confirm the previous studies employing FITC-dextran uptake by proximal tubules and its colocalization with CIC-5, although one investigation failed to colocalize CIC-5 with a fluid-phase marker of endocytosis using a permanent opossum kidney cell line (11).

The finding of an endocytosis defect in cyst-lining epithelial cells also raised the question of whether growth factors, which eventually could have an impact on cyst development, are affected by the endocytosis defect in proximal tubules. We were able to demonstrate that increased amounts of IGF-I, which probably do not originate in the kidney itself, are excreted by (*cy/+*) rats. Although no direct evidence has yet been presented that IGF-I contributes to cyst formation, IGF-I shows certain features that make it an interesting candidate. First, a previous report has presented evidence for the upregulation of IGF-I in the *pcy* mouse model of polycystic kidney disease (28). Second, binding studies (16, 18) and functional data (33) support the view that the receptor for IGF-I is located on both the apical and the basolateral side of proximal tubules. And, third, systemic administration of IGF-I results in a higher mitotic index in proximal tubules of rat kidneys (26) [an increased proliferation rate is also observed in polycystic kidneys (28, 34)]. Even if IGF-I did not play a key role in cyst formation, our study leaves open the possibility that other growth factors also accumulate in cyst fluid, which is one possible explanation for previous results showing that cyst fluid stimulates cell proliferation (47).

The importance of growth factors acting through the luminal side of cyst-lining epithelial cells is exemplified by epidermal growth factor (EGF). A relocation of the EGF receptor from the basolateral to the apical side of cyst wall epithelia has been repeatedly demonstrated (13, 32, 35, 39). The importance of these findings was emphasized by a study demonstrating that the expression of an EGF receptor mutant with decreased tyrosine kinase activity results in a significant decrease in cyst formation (35). Furthermore, the specific blockade of EGF receptor tyrosine kinase activity has recently been shown to reduce collecting duct cysts *in vitro* (41) and *in vivo* (40). In addition to the action of growth factors, proteinuria per se is supposed to aggravate tubulointerstitial disease (45), and some investigations also hint at a mitogenic role of albumin on proximal tubular cells in the pathophysiology of proteinuric states (12).

In summary, we have provided functional evidence that in the (*cy/+*) rat model of ADPKD, albuminuria and proteinuria result from the disappearance of components of the endocytic apparatus such as the chloride channel CIC-5 and the scavenger receptor megalin. This endocytic defect may play a secondary role in cyst development.

We thank Dennis Brown (Renal Unit, Massachusetts General Hospital, Charlestown, MA) for advice regarding the FITC-dextran studies. We are also thankful for the superb arrangement of the figures by Rolf Nonnenmacher and the expert photographic work of

Ingrid Ertel. Jutta Christophel skillfully performed the albumin ELISAs.

Parts of these studies were presented at the International Society of Nephrology Frontiers in Nephrology Symposium on Gene Therapy at Beaver Creek, CO (June 5–6, 2000).

REFERENCES

1. Adamo ML, Ben-Hur H, Roberts CT Jr, and LeRoith D. Regulation of start site usage in the leader exons of the rat insulin-like growth factor-I gene by development, fasting, and diabetes. *Mol Endocrinol* 5: 1677–1686, 1991.
2. Alt JM, Hackbarth H, Deereberg F, and Stolte H. Proteinuria in rats in relation to age-dependent renal changes. *Lab Anim Sci* 14: 95–101, 1980.
3. Ausubel FA, Brent R, Kingston RE, Moore DD, Seidman JG, Smith JA, and Struhl K. *Current Protocols in Molecular Biology*. New York: Wiley, 1996.
4. Bachinsky DR, Sabolic I, Emmanouel DS, Jefferson DM, Carone FA, Brown D, and Perrone RD. Water channel expression in human ADPKD kidneys. *Am J Physiol Renal Fluid Electrolyte Physiol* 268: F398–F403, 1995.
5. Blum WF and Breier BH. Radioimmunoassays for IGFs and IGFFBPs. *Growth Regul* 4, Suppl 1: 11–19, 1994.
6. Chapman AB, Johnson AM, Gabow PA, and Schrier RW. Overt proteinuria and microalbuminuria in autosomal dominant polycystic kidney disease. *J Am Soc Nephrol* 5: 1349–1354, 1994.
7. Chomczynski P and Sacchi N. Single-step method of RNA isolation by acid guanidinium thiocyanate-phenol-chloroform extraction. *Anal Biochem* 162: 156–159, 1987.
8. Cowley BD Jr, Gudapaty S, Kraybill AL, Barash BD, Harding MA, Calvet JP, and Gattone VH II. Autosomal-dominant polycystic kidney disease in the rat. *Kidney Int* 43: 522–534, 1993.
9. Cui S, Verroust PJ, Moestrup SK, and Christensen EI. Megalin/gp330 mediates uptake of albumin in renal proximal tubule. *Am J Physiol Renal Fluid Electrolyte Physiol* 271: F900–F907, 1996.
10. Devuyst O, Burrow CR, Smith BL, Agre P, Knepper MA, and Wilson PD. Expression of aquaporins-1 and -2 during nephrogenesis and in autosomal dominant polycystic kidney disease. *Am J Physiol Renal Fluid Electrolyte Physiol* 271: F169–F183, 1996.
11. Devuyst O, Christie PT, Courtoy PJ, Beauwens R, and Thakker RV. Intra-renal and subcellular distribution of the human chloride channel, CLC-5, reveals a pathophysiological basis for Dent's disease. *Hum Mol Genet* 8: 247–257, 1999.
12. Dixon R and Brunskill NJ. Activation of mitogenic pathways by albumin in kidney proximal tubule epithelial cells: implications for the pathophysiology of proteinuric states. *J Am Soc Nephrol* 10: 1487–1497, 1999.
13. Du J and Wilson PD. Abnormal polarization of EGF receptors and autocrine stimulation of cyst epithelial growth in human ADPKD. *Am J Physiol Cell Physiol* 269: C487–C495, 1995.
- 13a. The European Polycystic Kidney Disease Consortium. The polycystic kidney disease 1 gene encodes a 14 kb transcript and lies within a duplicated region on chromosome 16. *Cell* 77: 881–894, 1994.
14. Faraggiana T, Bernstein J, Strauss L, and Churg J. Use of lectins in the study of histogenesis of renal cysts. *Lab Invest* 53: 575–579, 1985.
15. Feld S and Hirschberg R. Growth hormone, the insulin-like growth factor system, and the kidney. *Endocr Rev* 17: 423–480, 1996.
16. Flyvbjerg A, Nielsen S, Sheikh MI, Jacobsen C, Ørskov H, and Christensen EI. Luminal and basolateral uptake and receptor binding of IGF-I in rabbit renal proximal tubules. *Am J Physiol Renal Fluid Electrolyte Physiol* 265: F624–F633, 1993.
17. Günther W, Lüchow A, Cluzeaud F, Vandewalle A, and Jentsch TJ. CLC-5, the chloride channel mutated in Dent's disease, colocalizes with the proton pump in endocytotically active kidney cells. *Proc Natl Acad Sci USA* 95: 8075–8080, 1998.
18. Hammerman MR and Rogers S. Distribution of IGF receptors in the plasma membrane of proximal tubular cells. *Am J Physiol Renal Fluid Electrolyte Physiol* 253: F841–F847, 1987.
19. Hartel-Schenk S, Gossrau R, and Reutter W. Comparative immunohistochemistry and histochemistry of dipeptidyl peptidase IV in rat organs during development. *Histochem J* 22: 567–578, 1990.
20. Kerjaschki D, Horvat R, Binder S, Susani M, Dekan G, Ojha PP, Hillemanns P, Ulrich W, and Donini U. Identification of a 400-kD protein in the brush borders of human kidney tubules that is similar to gp330, the nephritogenic antigen of rat Heymann nephritis. *Am J Pathol* 129: 183–191, 1987.
21. Lencer WI, Weyer P, Verkman AS, Ausiello DA, and Brown D. FITC-dextran as a probe for endosome function and localization in kidney. *Am J Physiol Cell Physiol* 258: C309–C317, 1990.
22. Lloyd SE, Pearce SHS, Fisher SE, Steinmeyer K, Schwappach B, Scheinman SJ, Harding B, Bolino A, Devoto M, Goodyer P, Rigden SPA, Wrong O, Jentsch TJ, Craig IW, and Thakker RV. A common molecular basis for three inherited kidney stone diseases. *Nature* 379: 445–449, 1996.
23. Lloyd SE, Pearce SHS, Günther W, Kawaguchi H, Igarashi T, Jentsch TJ, and Thakker RV. Idiopathic low molecular weight proteinuria associated with hypercalciuric nephrocalcinosis in Japanese children is due to mutations of the renal chloride channel (CLCN5). *J Clin Invest* 99: 967–974, 1997.
24. Maack T, Park CH, and Camargo MJF. Renal filtration, transport, and metabolism of proteins. In: *The Kidney: Physiology and Pathophysiology*, edited by Seldin DW and Giebisch G. New York: Raven, 1992, p. 3005–3038.
25. Marshansky V, Bourgoin S, Londoño I, Bendayan M, Maranda B, and Vinay P. Receptor-mediated endocytosis in kidney proximal tubules: recent advances and hypothesis. *Electrophoresis* 18: 2661–2676, 1997.
26. Mehls O, Irzyniec T, Ritz E, Eden S, Kovács G, Klaus G, Floege J, and Mall G. Effects of rhGH and rhIGF-1 on renal growth and morphology. *Kidney Int* 44: 1251–1258, 1993.
27. Mochizuki T, Wu G, Hayashi T, Xenophontos SL, Veldhuisen B, Saris JJ, Reynolds DM, Cai Y, Gabow PA, Pierides A, Kimberling WJ, Breuning MH, Deltas CC, Peters DJM, and Somlo S. *PKD2*, a gene for polycystic kidney disease that encodes an integral membrane protein. *Science* 272: 1339–1342, 1996.
28. Nakamura T, Ebihara I, Nagaoka I, Tomino Y, Nagao S, Takahashi H, and Koide H. Growth factor gene expression in kidney of murine polycystic kidney disease. *J Am Soc Nephrol* 3: 1378–1386, 1993.
29. Nykjaer A, Dragun D, Walther D, Vorum H, Jacobsen C, Herz J, Melsen F, Christensen EI, and Willnow TE. An endocytic pathway essential for renal uptake and activation of the steroid 25-(OH) vitamin D₃. *Cell* 96: 507–515, 1999.
30. Obermüller N, Gretz N, Kriz W, Reilly RF, and Witzgall R. The swelling-activated chloride channel CLC-2, the chloride channel CLC-3, and CLC-5, a chloride channel mutated in kidney stone disease, are expressed in distinct subpopulations of renal epithelial cells. *J Clin Invest* 101: 635–642, 1998.
31. Obermüller N, Gretz N, Kriz W, van der Woude FJ, Reilly RF, Murer H, Biber J, and Witzgall R. Differentiation and cell polarity during renal cyst formation in the Han:SPRD (cy/+) rat, a model for ADPKD. *Am J Physiol Renal Physiol* 273: F357–F371, 1997.
32. Orellana SA, Sweeney WE, Neff CD, and Avner ED. Epidermal growth factor receptor expression is abnormal in murine polycystic kidney. *Kidney Int* 47: 490–499, 1995.
33. Quigley R and Baum M. Effects of growth hormone and insulin-like growth factor I on rabbit proximal convoluted tubule transport. *J Clin Invest* 88: 368–374, 1991.
34. Ramasubbu K, Gretz N, and Bachmann S. Increased epithelial cell proliferation and abnormal extracellular matrix in rat polycystic kidney disease. *J Am Soc Nephrol* 9: 937–945, 1998.
35. Richards WG, Sweeney WE, Yoder BK, Wilkinson JE, Woychik RP, and Avner ED. Epidermal growth factor receptor activity mediates renal cyst formation in polycystic kidney disease. *J Clin Invest* 101: 935–939, 1998.

36. **Sakamoto H, Sado Y, Naito I, Kwon TH, Inoue S, Endo K, Kawasaki M, Uchida S, Nielsen S, Sasaki S, and Marumo F.** Cellular and subcellular immunolocalization of CIC-5 channel in mouse kidney: colocalization with H⁺-ATPase. *Am J Physiol Renal Physiol* 277: F957–F965, 1999.
37. **Schäfer K, Gretz N, Bader M, Oberbäumer I, Eckardt KU, Kriz W, and Bachmann S.** Characterization of the Han:SPRD rat model for hereditary polycystic kidney disease. *Kidney Int* 46: 134–152, 1994.
38. **Sharp C, Johnson A, and Gabow P.** Factors relating to urinary protein excretion in children with autosomal dominant polycystic kidney disease. *J Am Soc Nephrol* 9: 1908–1914, 1998.
39. **Sweeney WE Jr and Avner ED.** Functional activity of epidermal growth factor receptors in autosomal recessive polycystic kidney disease. *Am J Physiol Renal Physiol* 275: F387–F394, 1998.
40. **Sweeney WE Jr, Chen Y, Nakanishi K, Frost P, and Avner ED.** Treatment of polycystic kidney disease with a novel tyrosine kinase inhibitor. *Kidney Int* 57: 33–40, 2000.
41. **Sweeney WE, Futey L, Frost P, and Avner ED.** In vitro modulation of cyst formation by a novel tyrosine kinase inhibitor. *Kidney Int* 56: 406–413, 1999.
43. **Tönshoff B, Blum WF, Vickers M, Kurilenko S, Mehls O, and Ritz E.** Quantification of urinary insulin-like growth factors (IGFs) and IGF binding protein 3 in healthy volunteers before and after stimulation with recombinant growth hormone. *Eur J Endocrinol* 132: 433–437, 1995.
44. **Van Dijk MA, Peters DJM, Breuning MH, and Chang PC.** The angiotensin-converting enzyme genotype and microalbuminuria in autosomal dominant polycystic kidney disease. *J Am Soc Nephrol* 10: 1916–1920, 1999.
45. **Williams JD and Coles GA.** Proteinuria—a direct cause of renal morbidity? *Kidney Int* 45: 443–450, 1994.
46. **Willnow TE, Goldstein JL, Orth K, Brown MS, and Herz J.** Low density lipoprotein receptor-related protein and gp330 bind similar ligands, including plasminogen activator-inhibitor complexes and lactoferrin, an inhibitor of chylomicron remnant clearance. *J Biol Chem* 267: 26172–26180, 1992.
47. **Yamaguchi T, Nagao S, Takahashi H, Ye M, and Grantham JJ.** Cyst fluid from a murine model of polycystic kidney disease stimulates fluid secretion, cyclic adenosine monophosphate accumulation, and cell proliferation by Madin-Darby canine kidney cells in vitro. *Am J Kidney Dis* 25: 471–477, 1995.
48. **Zor T and Selinger Z.** Linearization of the Bradford protein assay increases its sensitivity: theoretical and experimental studies. *Anal Biochem* 236: 302–308, 1996.

